Journal of Nuclear Materials 438 (2013) S655–S658

Contents lists available at SciVerse ScienceDirect

Journal of Nuclear Materials

journal homepage: www.elsevier.com/locate/jnucmat

Chemical sputtering studies of lithiated ATJ graphite ☆

P. Raman, A. Groll, P. Fiflis, D. Curreli, D. Andruczyk *,[1], D.N. Ruzic

Center for Plasma–Material Interactions, Department of Nuclear, Plasma and Radiological Engineering, University of Illinois at Urbana Champaign, Urbana, IL 61801, USA

ARTICLE INFO

Article history:
Available online 17 January 2013

ABSTRACT

Lithium evaporation treatments in the National Spherical Torus Experiment (NSTX) have shown dramatic improvements in plasma performance increasing the viability of lithium as a Plasma Facing Component (PFC) material. In order to understand the complex system of lithiated ATJ graphite, chemical sputtering measurements of plain and lithiated ATJ graphite are conducted in our upgraded IIAX (Ion Surface Interaction Experiment) facility with a differentially pumped Magnetic Sector Residual Gas Analyzer (MSRGA). Chemical sputtering of graphite is dependent on the ion energy and substrate temperature, hence the effects of treating ATJ graphite with lithium in hydrogen plasma is investigated in terms of different target temperatures and bias voltages. For this purpose, lithium was evaporated in situ onto ATJ graphite and chemically sputtered species in hydrogen plasma were measured using MSRGA. The dominant chemical sputtering product was CH_4. Initial experiments show that lithium treatments have suppressed the chemical sputtering of ATJ graphite.

1. Introduction

Plasma Facing Component (PFC) materials are critical to fusion reactor development. There is no one material that functions as an ideal PFC material [5]. Graphite is the usual choice for divertor and first wall material due to its low *Z* number and its better thermal, chemical and thermomechanical properties [1]. However graphite suffers from chemical erosion due to its reactivity with hydrogen isotopes [2]. ATJ graphite tiles are currently used in the National Spherical Torus Experiment (NSTX) as Plasma Facing Components (PFCs). Previous studies show that the deposition of a thin layer of lithium on graphite walls dramatically suppresses the release of carbon impurities at room temperature [3]. Chemical erosion of carbon by hydrogen is a thermally activated process which does not require energetic species whereas chemical sputtering is a process whereby ion bombardment causes or allows a chemical reaction to occur which produces a particle that is weakly bound to the surface and easily desorbed into the gas phase [5]. Chemical sputtering includes all three basic erosion mechanisms like chemical erosion, physical sputtering, and chemical sputtering [6]. It is hard to pin point which mechanism dominates as their extent of influence depends on experimental parameters like ion energy and the temperature of the sample. Chemical sputtering shows strong temperature dependence significantly below melting or sublimation temperatures [6]. Qualitatively, lithium treatments on ATJ graphite have shown to suppress chemical erosion products [4]. This research focuses on understanding the effects of lithium on chemical sputtering of ATJ graphite. Usually, beam irradiation with a heated target is used in studying chemical sputtering characteristics. However, a low energy hydrogen RF plasma with a heated ATJ target is used in IIAX at the University of Illinois for this study. IIAX has been modified to study the chemical sputtering suppression due to in situ lithium evaporation, so the percentage of suppression from plain ATJ to lithiated ATJ graphite is exactly determined. The erosion/sputtering products are methane, ethane, propane, etc. However, the major contribution to the chemical sputtering comes from single chained hydrocarbons. The emission of hydrocarbons of lengths 2 and 3 is more than one order of magnitude smaller and due to their interference with more dominant species like carbon monoxide and carbon dioxide [7] and will not be considered in the analysis.

2. Experimental details

2.1. Experimental set-up

Mass spectrometry is one of the most popular methods in measuring chemical sputtering. An advantage of mass spectrometry is that it produces real-time data and allows measuring parameter variations in much shorter times [6]. A differentially pumped low-mass-sensitive Magnetic Sector Residual Gas Analyzer (MSRGA) was used in this study to track the chemical sputtering products. The hydrogen RF plasma used in this study required the chamber pressure to be at a few millitorr which is not a

☆ Work is supported by Department of Energy/ALPS Contract: DEFG02-99ER54515.

* Corresponding author. Address: 216 Talbot, 104 S. Wright St., Urbana, IL 61801, USA.

E-mail addresses: druzic@illinois.edu, andruczy@illinois.edu (D. Andruczyk).

[1] Presenting author.

0022-3115/$ - see front matter © 2013 Elsevier B.V. All rights reserved.
http://dx.doi.org/10.1016/j.jnucmat.2013.01.138

suitable condition to operate a RGA. Therefore, the MSRGA was attached to a differentially pumped remote chamber which was connected to the experimental chamber with an orifice in between them. In order to detect the reaction products, MSRGA needed to be placed in the line of sight of the origin of those products. This was achieved by installing a differentially pumped sniffer tube close to the target. This tube captured the produced reaction products. Line-of-sight setup is necessary but not sufficient to detect reactive species and that significant effort has to be spent to reduce the signal contribution of recycling species from the background [6]. The experimental set-up consists of two chambers, IIAX chamber where the actual reactions take place and the remote sampling chamber where the line of sight MSRGA was attached to monitor the reaction species. The remote sampling chamber is connected to the IIAX chamber using a sniffer tube with an orifice. An orifice is very critical for differential pumping and that is where the line of sight sputtering products entered the sampling chamber and eventually made their way to the MSRGA. The experimental IIAX set-up consisted of a RF coil, a movable cylindrical ATJ graphite target of 2.5 cm diameter, an in situ lithium evaporator, and a bake lamp underneath the target to heat the ATJ graphite target. The ATJ graphite target was mounted in such way that the target could be translated along a line to different positions. Here it was either under the coil facing sniffer tube, in front of the evaporator, or away from the line of sight of the sniffer tube to evaluate contributions from these different locations. The target could also be rotated to expose the plain ATJ surface or lithiated ATJ surfaces to the sniffer tube which allows direct comparison of both sides with the same background. Thermocouple and biasing connections were attached to the target to monitor the temperature and bias the target. Fig. 1 shows the upgraded IIAX chemical sputtering detection set-up. This type of set-up enabled us to get exact quantitative measure of chemical sputtering suppression due lithium. Plasma was produced in the main chamber using RF antenna coil when the pressure in the main chamber reached the millitorr range with the hydrogen gas flow. To maintain a constant gas flow during all experiments, a mass flow controller was used to regulate the flow of hydrogen into the chamber.

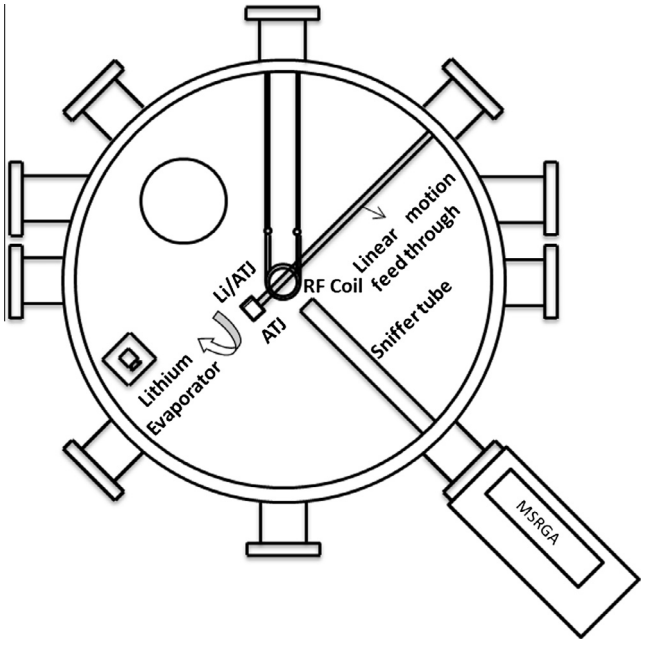

Fig. 1. Schematic of the IIAX chemical sputtering detection set-up.

2.2. Cracking pattern generation

When molecules of a gas are struck by energetic electrons they cause ionization and fragments of several mass-to-charge ratios are created. The mass-to-charge values are unique for each gas species and the peak amplitudes are dependent on the gas and instrumental conditions [8]. This pattern of fragments is called a cracking pattern. They form a fingerprint that may be used for absolute identification of a gas. Cracking pattern of gases depend on the type of the gas analyzer used, location of the analyzer, purity of the gases analyzed, detection mode of the analyzer, purity of the analyzer filament and the sensitivity of the analyzer. Cracking patterns were obtained for our MSRGA according to our set-up and experimental conditions. Specific amount of gases were let into the chamber and their cracking ratios at the MSRGA were recorded. The matrix formed from these cracking pattern ratios was used to find the actual partial pressures of the species considered in the analysis. The experiments were preformed multiple times and the standard deviations for each of the component coefficients were established. Those standard deviations were then used for error propagation. Cracking pattern of methane, hydrogen, water vapor, oxygen, nitrogen, argon and carbon dioxide were generated. These specific gases were chosen because of their interference with the methane cracking pattern. Table 1 shows the cracking pattern matrix with standard deviations from our cracking pattern analysis. For example, methane cracks from masses 12 to 16 which correspond to the species like C, CH, CH_2, CH_3 and CH_4. Nitrogen cracks at 14 and 28. The partial pressure at peak 14 has contribution from methane as well as nitrogen. In order to de-convolute the signals and find the contribution of the desired species, it was essential considering all the interfering species in the analysis.

2.3. Chemical sputtering experiment

Two different experiments were conducted for different target orientation with three different biasing conditions (0 V, −1000 V and −2000 V) and three different target temperatures (300 K, 373 K and 453 K), as discussed below:

1. With the ATJ graphite target under the RF coil facing the sniffer tube to capture line of sight chemically sputtered species in a pure non-lithiated environment.
2. With the ATJ graphite target under the RF coil facing the sniffer tube after one side of the target was coated with lithium.
3. With the Li/ATJ graphite target under the RF coil facing the sniffer tube to study the effect of lithium treatments on chemical sputtering. For this measurement, lithium was evaporated in situ onto graphite using a lithium evaporator for 5 min. Lithium deposition thickness on silicon witness plate was found to be 150 nm using DEKTAK profilometer.
4. With the target in a far away position from the sniffer tube to measure the baseline or wall contribution for getting more information on our wall conditions.

A 10 W hydrogen RF plasma is ignited using a RF power supply. Usually for plasma based experiments, methane from the chamber walls dominate the methane contribution from the actual target. Using a higher RF power will increase the wall contribution, a lower power is used to decrease the plasma from spreading throughout the chamber. Biasing in addition to low power enables the plasma to be focused onto the target area. In order to reduce the wall contribution a high power argon/oxygen plasma cleaning was done to the IIAX chamber before the start of the experiments. The MSRGA was used to monitor the partial pressures of selected masses in 1–50 amu range in the sampling chamber. The MSRGA also allows us to monitor the partial pressures of selected mass

Table 1
Cracking pattern matrix of different gases.

Mass	CH_4	H_2O	N_2	O_2	CO_2	Ar	H_2
1	0.182 ± 0.028	0.486 ± 0.006	0	0	0	0	0.087 ± 0.078
2	0.182 ± 0.028	0.486 ± 0.006	0	0	0	0	0.456 ± 0.388
3	0.007225	0					0.456
12	0.013 ± 0.002	0	0	0	0.152 ± 0.001	0	0
13	0.025 ± 0.001	0	0	0	0	0	0
14	0.182 ± 0.025	0	0.133 ± 0.007	0	0	0	0
15	0.203 ± 0.017	0	0	0	0	0	0
16	0.203 ± 0.017	0	0	0.229 ± 0.017	0.246 ± 0.004	0	0
17	0	0.013 ± 0.006	0	0	0	0	0
18	0	0.013 ± 0.006		0	0	0	0
20	0	0	0	0	0	0.379 ± 0.003	0
22	0	0	0	0	0.017	0	0
28	0	0	0.866 ± 0.007	0	0.092 ± 0.001	0	0
32	0	0	0	0.770 ± 0.017	0	0	0
40	0	0	0	0	0	0.620 ± 0.003	0
44	0	0	0	0	0.490 ± 0.002	0	0

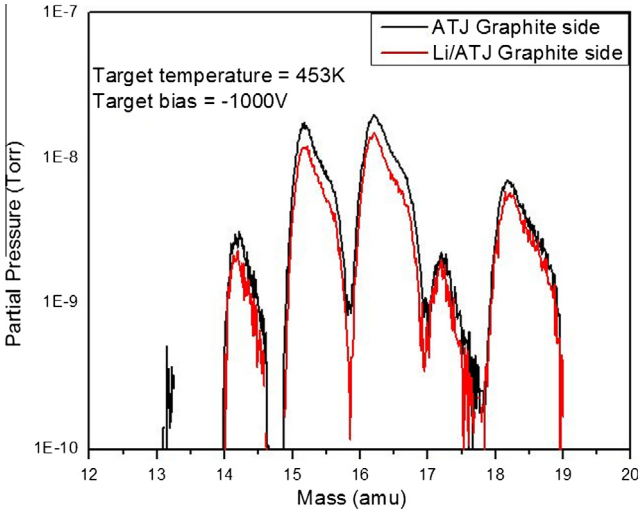

Fig. 2. Overlay of two MSRGA scans obtained by rotating the target for the side exposed to lithium evaporation to the side that was not covered for the case of 453 K target temperature and −1000 V target bias.

peaks versus exposure time (*P* versus *T* scans), which enables us to determine the steady conditions. The scans were collected only after steady state conditions were reached (usually a couple of minutes). The small transient was due to moving the linear feedthrough or immediate outgassing of the RF antenna. Multiple RGA scans were collected at each condition to determine the standard deviation of partial pressures at specific masses which was used for error propagation.

Fig. 2 shows the overlay of two MSRGA scans obtained by simply rotating the target for the side exposed to lithium evaporation to the side that was not covered for the case of 453 K target temperature and −1000 V bias. The hydrogen plasma was kept on for both measurements.

2.4. Data analysis and error propagation

Chemical sputtering products were determined by a matrix inversion approach. The RGA signals at specific masses from the lithiated ATJ case were subtracted from the ATJ case directly due to ability of our set-up as both have the same background contributions. The partial pressures of the desired species for example methane can be calculated from the formula $C * S = p$. *Where C* represents our cracking pattern. *S* represents the partial pressures at specific masses and *p* is the partial pressures of the desired species. The specific partial pressure signals were multiplied with the inverse of the corresponding cracking pattern matrix to obtain the individual partial pressures of the desired chemical erosion species which is methane in our case. Five linear equations were used in this analysis. The species included in the analysis are CH_4, H_2O, N_2, O_2 and CO_2 .The error in calculating the partial pressures of methane in our analysis is determined by classical McClintock formula. The equation for calculating methane is given by

$$S_{15} = a_{15} P_{CH_4}$$
$$P_{CH_4} = S_{15}/a_{15}$$
$$\Delta P_{CH_4} = \sqrt{\left(\left(\frac{1}{a_{15}}\right)^2 (\Delta S_{15})^2 + \left(\frac{S_{15}}{a_{15}^2}\right)^2 (\Delta a_{15})^2\right)}$$

S_{15} represents the mean value of signal at mass 15. P_{CH_4} is the partial pressure of methane, a_{15} is the mean cracking pattern ratio of methane at mass 15 which is obtained from the cracking pattern analysis, ΔS_{15} represents the standard deviation of signal at mass 15, Δa_{15} is the standard deviation of cracking pattern ratio of methane at mass 15. ΔP_{CH_4} is the absolute error in calculating methane. Signal at peak 15 was used in determining partial pressure of methane because of its high signal intensity at that mass which leads to lower error value. The error in temperature measurement will be incorporated in the upcoming experiments.

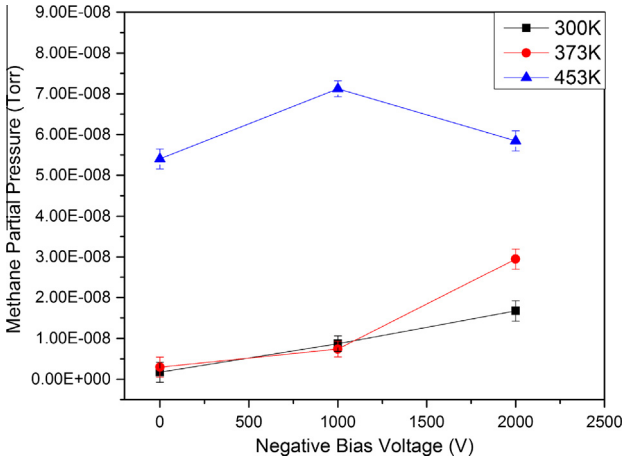

Fig. 3. Partial pressures of methane from ATJ target as a function of hydrogen ion energy at different sample temperatures in a pure nonlithium environment.

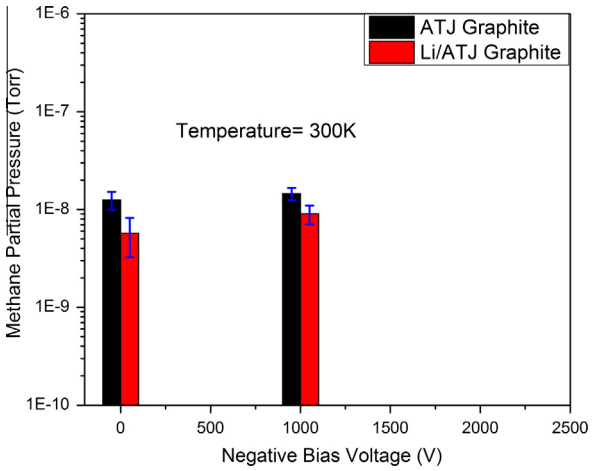

Fig. 4. Comparison of methane partial pressures at 300 K for ATJ target and lithiated ATJ target at different bias voltages.

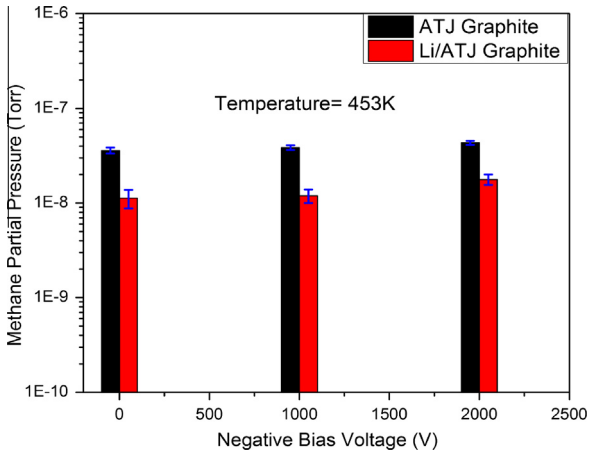

Fig. 5. Comparison of methane partial pressures at 453 K for ATJ target and lithiated ATJ target at different bias voltages.

2.5. Results and discussion

A series of experiments were conducted in order to study the effect of lithium on the chemical sputtering of ATJ graphite in a hydrogen plasma under different biasing and heating conditions. The data analysis was done based on the procedure explained in the previous section. Fig. 3 shows a plot of the methane partial pressures from the pure ATJ target as a function of different target bias conditions at different target temperatures in a non-lithiated environment. It can be clearly seen from the plot that as the temperature increases from 300 K to 453 K, the methane production also increases and has strong dependence on the target biasing voltage. A distinct maximum occurs around −1000 V for high temperatures. At higher biasing voltages, the methane partial pressure decreases for higher temperatures. This behavior is very similar to the trend from Yamada et al. [9], where the methane yield increased as the temperature increased and a maximum yield was observed for 1000 eV hydrogen ion impinging energies. They too saw a drop in methane yield past the 1000 eV threshold. Fig. 4 is a plot of methane partial pressures at 300 K for ATJ target and lithiated ATJ target at different bias voltages. At room temperature, lithium suppresses chemical sputtering but at higher values of bias the effect is less pronounced. Fig. 5 is a plot of methane partial pressures at 453 K for ATJ target and lithiated ATJ target at different bias voltages. Chemical sputtering and suppression effect can be clearly observed at higher temperatures since chemical sputtering has a strong dependence on temperature and ion energies. As expected from these plots, the chemical sputtering suppression effects of lithium at different bias voltages is more pronounced at higher temperatures and the resulting numbers also indicate the same. Table 2 shows the percentage of chemical sputtering due to lithium deposition for different bias voltage at 453 K. From the initial set of experiments, it can be concluded that lithium treatments suppress the chemical sputtering of graphite. Lithium coating thickness definitely plays a role in the chemical sputtering suppression. Different thickness of lithium will be deposited onto ATJ graphite to better understand the suppression phenomenon.

Table 2
Chemical sputtering suppression due to lithium coating at 453 K target temperature.

Bias voltage	Methane partialpressure (Torr)		Suppression (%)
	ATJ	Li/ATJ	
0	3.6E−08 ± 1.8E−09	1.1E−08 ± 5.6E−10	69 ± 10
1000	3.9E−08 ± 1.9E−09	1.2E−08 ± 6.0E−10	69 ± 10
2000	4.3E−08 ± 2.2E−09	1.8E−08 ± 8.9E−10	59 ± 8

3. Summary and conclusions

A simple experimental and mathematical approach that includes only single-carbon hydrocarbons is presented here. The species that were included in the analysis are CH_4, H_2O, N_2, O_2 and CO_2. The ability to rotate the target in front of the "sniffer" tube from a bare graphite side to a lithium-coated graphite side allows direct comparison with the same background. In situ lithium evaporation, a RF plasma source and a bias-able target are critical experimental components. Lithium deposition on ATJ graphite shows the suppression of methane from the initial set of experiments. The chemical erosion studies conducted in a plasma chamber, as opposed to beam experiments, provide a better understanding of the phenomenon taking place in tokamaks. More experiments will be done with varying lithium thickness to determine the threshold level for suppression. Chemical sputtering measurements, as a function of different lithium thicknesses, are in progress.

Acknowledgements

This work is supported by DOE Contract DE-FG02-04ER54765. The authors would like to thank Mike Williams for help with experimental set up, Dr. M. Neito for technical discussions.

References

[1] Graphite in High Power Fusion Reactors, in: W.V. Green, S.L. Green, M. Victoria, (Eds.), IEA Workshop Report Rigi Kaltbad, Switzerland, October 1982.
[2] J. Roth, W. Möller, Nucl. Instrum. Methods B 7/8 (1985) 788.
[3] H. Sugai, M. Ohori, H. Toyoda, Vacuum 47 (1996) 981.
[4] V. Surla, P. Raman, D. Burns, M.J. Neumann, D.N. Ruzic, J. Nucl. Mater. 415 (2011) S174–S178.
[5] H.F. Winters, J.W. Coburn, Surf. Sci. Rep. 14 (1992) 161.
[6] R. Behrisch, W. Eckstein (Eds.), Sputtering by Particle Bombardment. Experiments and Computer Calculations from Threshold to MeV Energies, Springer, Berlin, 2007.
[7] M. Nieto-Perez, J.P. Allain, C.B. Heim, C.N. Taylor, J. Nucl. Mater. 415 (2010) S133–S136.
[8] John F O'Hanlon, A User's Guide to Vacuum Technology, third ed., Wiley-Interscience, 2003, ISBN: 0471270520M.
[9] R. Yamada, K. Nakamura, K. Sone, M. Saidoh, J. Nucl. Mater. 95 (1980) 278.